High-efficient long spin coherence electrical spin injection in CoFe/InGaAs two-dimensional electron gas lateral spin-valve devices

Shiro Hidaka, Masashi Akabori, and Syoji Yamada*

Center for Nano Materials and Technology (CNMT),
Japan Advanced Institute of Science and Technology (JAIST)

1-1, Asahi-dai, Nomi, Ishikawa 923-1292, Japan.

*Correspondence to: shooji@jaist.ac.jp

Electrical spin injection experiments are performed at 1.5 K in a new hybrid structure, $In_{0.75}Ga_{0.25}As$ two-dimensional electron gases (2DEGs) with lateral $Co_{0.8}Fe_{0.2}$ electrodes. From the electrode spacing ($\leq$ ~9 μm) dependence of the spin-valve signals in non-local regime, we obtained very promising results such as longer spin diffusion length L_S of ~ 5.1 μm and higher spin polarization η of ~5.7 % than those in the former reports. They are mainly attained by the suppression of D'yakonov-Perel' spin relaxation process due to the tuned spin-orbit (SO) interactions.

Semiconductor (SC) spintronics [1] has the affluent potential to overcome a variety of limitations in conventional SC electronic devices. Among the problem of spin polarized current (or charge) injection into SC [2], in non-magnetic (NM) SC spintronics, where the base material is not a dilute magnetic semiconductor (DMS) [3] but some bulk or hetero-junction materials with specific spin control effects [4], *electrical* spin injection from ferromagnetic metals (FMs) is a challenge to realize *practical* spintronics devices. Recently, there have been a lot of reports on electrical spin injection using *non-local* (NL) spin-valve (SV) measurement [5, 6], since it can greatly suppress the influence of anisotropic magneto-resistance (AMR) [7] and local Hall effect (LHE) [8, 9]. Additionally, the sample structures have also been improved to suppress the impedance mismatch [10] by using the insulating tunnel barriers between FM and SC, the FM/SC Schottky contacts with highly-doped SC thin-layers, and the combination of insulating tunnel barriers and highly-doped SC thin bulk layers of GaAs [11, 12] and Si [13. 14].

Different kind NM spintronics model device is a spin -FETs [15] utilizing Rashba type SO coupling (Rashba-SOC) [16] as an operating principle. The 2DEG material systems with $In_xGa_{1-x}As$ have been studied widely and extensively for the decade. We have especially focused on $In_{0.75}Ga_{0.25}As$ / $In_{0.75}Al_{0.25}As$ 2DEGs, since it shows a very high electron mobility (< ~3×10^5 cm^2/Vsec) as well as a very strong Rashba-SOC (< ~25×10^{-12} eVm) [17, 18] at low temperatures. Due to those properties, we have studied also electrical spin injection experiments into the $In_{0.75}Ga_{0.25}As$ 2DEGs from NiFe electrodes [19-21], although they were carried out based on the local SV configurations and only a few percent spin injection efficiencies (η) were confirmed. As for the NLSV measurement in a similar material system ($Ni_{0.81}Fe_{0.19}$-$In_{0.53}Ga_{0.47}As$/InAs 2DEG), Koo et al [22] have reported L_S = 1.8 μm and η= 1.9 % as well as the interface resistance (R_I) dependency including the case of Co electrodes [23]. In the works, however, very thin (a few nm) and hence difficult to control interface layer were

reported and the very small interface resistances, R_Is, were also assigned. This small R_I means also that the impedance mismatch theory [12] was not appropriate in their case.

In this work, in a new structure composed of inverted $In_{0.75}Ga_{0.25}As$-2DEGs (channel thickness of 40 nm) and $Co_{0.8}Fe_{0.2}$ electrodes, we report the alternative electrical spin injection experiments performed under the similar NL SV configurations. Here we have *not* carried out any nm-scale control of the InGaAs interface layer between the 2DEG and the CoFe electrodes, since it is often less reproducible due to the oxidized layer in the ex-situ process. We then confirmed much improved (almost three times larger) spin dependent parameters such as L_S = ~5.1 μm in the 2DEG and η = ~5.7 % at the FM-2DEG interface when compared with the former works. Those parameters seem, however, inconsistent with the results (L_{SO} etc) obtained in the weak anti-localization (WAL) experiment done separately. As one of the possible origin which could give such excellent parameters much deviated from the WAL ones, a suppression mechanism of the D'yakonov-Perel' spin relaxation process in the 2DEG is then discussed.

The present $In_{0.75}Ga_{0.25}As$ 2DEG wafer is an inverted $In_{0.75}Ga_{0.25}As/In_{0.75}Al_{0.25}As$ modulation-doped heterostructure with 40-nm $In_{0.75}Ga_{0.25}As$ channel layer at the top surface. This is grown on a semi-insulating GaAs (001) substrate via $In_yAl_{1-y}As$ (y = 0.15-0.8) metamorphic step graded buffer layers by a conventional solid-source molecular beam epitaxy [21]. Since Si delta-doping layer is located at the substrate side from the 2DEG channel, there are no doping nor barrier layers between the surface and the 2DEG interface.

From the magneto-resistance signals including Shubnikov-de Haas oscillation, we obtained sheet electron concentration, $n_S = 6.4\times10^{11}$ cm^{-2} and electron mobility, μ_e = 44,000 cm^2/V·s at 1.5 K. From the WAL measurement, we obtained Rashba-SOC constant $\alpha = 5.1\times10^{-12}$ eV·m at 1.5 K by the fitting with the Iordanskii, Lyanda-Geller, and Pikus (ILP) model [24]. The spin

relaxation time τ_{SO} by D'yakonov-Perel' (DP) mechanism [25] is estimated to be 0.4 psec from the equation $\tau_{SO} = eh^2/(2\pi\alpha k_F)^2 m^* \mu_e$, where $k_F = (2\pi n_S)^{1/2}$ is the Fermi wave number, and m^* (~$0.04m_0$) is an 2DEG effective mass. The spin diffusion length $L_{SO} = (D_e\tau_{SO})^{1/2}$ is also estimated to be 0.2 μm. Here, the diffusion coefficient $D_e = v_F^2\tau_{tr}/2$ is determined by the electron transport properties; $v_F = \hbar k_F/m^*$ is a Fermi velocity, and $\tau_{tr} = m^*\mu_e/e$ is a momentum relaxation time.

Figures 1(a) and (b) show an optical microscope image and a schematic illustration of fabricated SV device with NL SV and three-terminal (3T) measurement geometries, respectively. We fabricated three samples having different range of electrode spacing L. Different magnetization behaviors of $Co_{0.8}Fe_{0.2}$ electrodes (parallel or anti-parallel status) can be controlled by the difference in length of $Co_{0.8}Fe_{0.2}$ electrode pair (1 μm-long and 3 μm-long) for NL SV measurements. The fabrication process of the SV devices is described as follows: The 2DEG mesas (50 μm-wide, 300 μm-long, and 300 nm-height) were formed by electron-beam (EB) lithography and sulfuric-acid-based wet-etching. Finally, 30 nm-thick $Co_{0.8}Fe_{0.2}$ electrodes overlapping the 2DEG mesa edges were formed by EB lithography, RF magnetron sputtering and lift-off. In order to remove the native oxide underneath the $Co_{0.8}Fe_{0.2}$ electrodes, a wet process was adopted just prior to the sample loading into the RF sputtering chamber. The NL resistance $R_{NL} = V_{NL}/I_{AC}$ was measured while sweeping the in-plane magnetic fields B in the longitudinal direction of the $Co_{0.8}Fe_{0.2}$ electrode by standard low-frequency AC lock-in method in ^{4}He cryostat with a superconducting magnet. The amplitude of AC current I_{AC} was 1 μA rms, the DC bias current I_{DC} was 10 μA (i.e., total injected current I_{NL} is $I_{DC} + I_{AC}$) and the current direction was fixed in the direction of [1-10].

Figure 2 (a) shows the NL resistance R_{NL} curves in L = 1.0, 3.0 and 8.5 μm as a function of B (10 sweeps averaged) obtained from the three samples. The clear SV behaviors of R_{NL} with

peaks at ~ ± 40 mT were observed and they were almost identical when we exchanged the current and voltage terminals between the two FM electrodes. We consider this reason later. Such SV behaviors of R_{NL} are considered to be an evidence of successful spin injection and detection in $Co_{0.8}Fe_{0.2}/In_{0.75}Ga_{0.25}As$-2DEG system. Relatively high baselines for the SV signals are found in Fig. 2 (a). This is the similar feature often observed in semiconductor SV systems [26]. At present, we consider that this can be attributed to the relatively high interface resistances (R_Is) (shown later) between the FM electrodes and the 2DEG, that is, the resistance of the bulk thin $In_{0.75}Ga_{0.25}As$ layer. Those high baselines probably arises due to the partial penetration of electric lines of force from the injector FM electrode into the region under the detector FM electrode in the NL SV measurement. In fact, the absolute value of the baseline decreased with increase of L, the distance between the FM electrodes.

Figure 2 (b) shows I-V characteristics of $Co_{0.8}Fe_{0.2}$–$In_{0.75}Ga_{0.25}As$ interface at 1.5 K and B=0 T obtained by the 3T measurements as schematically shown in Fig. 1(b). In spite of the low measurement temperatures, the I-V curves were almost linear. Tunnel effects at the $Co_{0.8}Fe_{0.2}$ –$In_{0.75}Ga_{0.25}As$ interface can therefore be negligible in our samples as in Ref. [22]. From the I-V curves, we can estimate the $R_{3T} = R_I$ values as ~300 and ~900 Ω for the FM electrodes with lengths of 3 and 1 μm, respectively. We then finally evaluated interface resistance-area product R_IA of the $Co_{0.8}Fe_{0.2}$–$In_{0.75}Ga_{0.25}As$ interface to be typically ~40 kΩ·μm^2, which is one or two orders higher than the former values [23].

In Fig. 3 (a), the 3T resistances ($R_{3T} = R_I$) for the two FM electrodes measured again in the configuration in Fig. 1(b) as a function of B, which usually reflect the AMR signals or the hysteresis nature of the FM electrodes, are shown and compared with the R_{NL} signal (L = 1 μm case). Note here that all the three kind signals are represented as the difference between the up-sweep and down-sweep curves for clarifying the fine structure of the signals. As seen in the

figure, it is almost confirmed that the two SV peaks of (R_{NL}(up) - $R_{NL(down)}$) appear between the peaks of the (R_{3T}(up) - $R_{3T(down)}$) signals from the short (1 μm) and long (3 μm) FM electrodes. In other words, the SV peaks seem to locate in between the fields of the two coercive forces of the CoFe electrodes. This means that the signals in Fig. 2 (a) can indeed be attributed to the anti-parallel magnetization state of the two FM electrodes, that is, the SV effect itself [26].

Figure 3 (b) shows R_{NL} peak height change ΔR_{NL} as a function of L. ΔR_{NL} was defined as a half magnitude (a half of the difference between the maximum and minimum of R_{NL}) of $|R_{NL(up)} - R_{NL(down)}|$ curve. The ΔR_{NL} seems to be exponentially decayed with increasing L, and this result agrees well with a following phenomenological expression of spin accumulation at the interface [8];

$$\Delta R_{NL}(L) = (\eta^2 \rho_S L_S / W) \exp [-L / L_S], \quad (1)$$

where η is a spin polarization at L = 0, $\rho_S = (en_s\mu_e)^{-1}$ is a sheet resistance of the 2DEG, L_S is a polarized-spin diffusion length, and W is an $In_{0.75}Ga_{0.25}As$-2DEG mesa width. From the fitting line in Fig. 3 (b), L_S and η were estimated to be ~ 5.1 μm and ~ 5.7 %, respectively. Additionally, polarized-spin relaxation time τ_S is estimated to be ~0.16 nsec by using $L_S = (D_e\tau_S)^{1/2}$. From this η value and a literature value of spin polarization in a similar CoFe alloy composition [27], spin injection efficiency of *~11 %* was obtained. These values are much larger than those in a similar $Ni_{0.81}Fe_{0.19}$-$In_{0.53}Ga_{0.47}As$/InAs composite system at 20 K (L_S = 1.8 μm, η ~ 1.9 %, and τ_S ~ 5 psec at 20 K) [22]. Here, we consider the spin resistance, R_s, discussed in the works by S. Takahashi et al [28] and T. Kimura et al [29]. By using the equation of $R_S = L_S\rho_S / W$ and the L_S value obtained above, we get R_S ~ 23 Ω for our system. This is one order larger than that of Cu ~ 2.6 Ω [30]. This difference suggests the robust spin relaxation process in our spin-injection system when compared with the Cu case. However, the R_S value is still one or two orders smaller than R_Is (300 or 900Ω) in our system. Since $R_S << R_I$s,

the interface might be regarded as “tunnel-like” rather than “ohmic”. This would be the main reason that the SV results did not sensitive to the FM electrode exchange.

The most possible origin of the much larger spin parameters obtained in our NL SV experiment and of the discrepancy from those in WAL analysis seems to be related to the condition of persistent spin helix (PSH) [31], in which the Rashba and Dresselhaus SOCs are coexisting in the similar strengths with each other. In such a case, Rashba type spin precession is suppressed and longer L_S would be attained. In our experiments, the 2DEG wafer with moderate (rather small) value of $\alpha \sim 5\times10^{-12}$ eVm is selected, although the largest value of α in $In_{0.75}Ga_{0.25}As$ 2DEG reaches up to $\sim25\times10^{-12}$ eVm [21]. The SO constant (β) of the linear Dresselhaus term, which is inversely proportional to the 2DEG distribution within the well, seems rather small due to the wide $In_{0.75}Ga_{0.25}As$ triangular quantum well in our sample. Our rough estimation gives, however, a value of $\beta < \sim 3\times10^{-12}$ eVm and in this sense the possibility of occurring near PSH condition ($\alpha \sim \beta$) in our sample is not excluded entirely. In contrast, the α value in the $In_{0.53}Ga_{0.47}As$-InAs well in Ref. 22 is $\sim10\times10^{-12}$ eVm and it could lead to the condition of even far from the PSH. The much longer L_S in our work can be explained by this difference in α. We finally describe that the SV behaviors in our samples are found to survive over several tens K. This seems reasonable, since both the SOI depends on the structure parameters (interface electric field in Rashba and confining well width in Dresselhaus cases, respectively) only and thus they could have no temperature dependencies.

We have demonstrated clear spin injection and detection in $Co_{0.8}Fe_{0.2}$-$In_{0.75}Ga_{0.25}As$ 2DEG system with strong Rashba-SOC using LSV devices under NLSV geometry. We obtained $L_S \sim$ 5.1 μm for the spin diffusion length, $\eta \sim 5.7$ % for the spin polarization at $L = 0$ and $\tau_S \sim 0.16$ nsec (spin relaxation time) from the L (electrode distance) dependency of the R_{NL} obtained in

NLSV measurements. These values are much improved than those reported recently in a similar $Ni_{0.81}Fe_{0.19}$-$In_{0.53}Ga_{0.47}As$/InAs system and world recordable suggesting the promising features in this material system. The extension of L_S and enhancement of η seem to be brought about by the suppression of the spin relaxation process by the Rashba SOC possibly due to the near PSH condition on the basis of the moderate value of the SOC. This means more easy realization of the Datta-Das spin-FET operation as not a ballistic device but a diffusive one.

Acknowledgments:

This work is partially supported by JST ALCA (Advanced Low Carbon Technology R&D program) grant.

References

[1] D. D. Awschalom, D. Loss, N. Samarth, *Semiconductor Spintronics and Quantum Computation*, Springer Berlin, (2002).

[2] Chapters 2 and 3 in Ref. [1]; S. Murakami, N. Nagaosa and S. –C. Zhang, Science **301** (2003) 1348.

[3] H. Ohno: Science, **281** (1998) 951, T. Dietl, H. Ohno, F. Matsukura, J. Cibert and D. Ferrand: Science, **287** (2000) 1019.

[4] For example, nuclear spins are treated in D. D. Awschalom and J. Kikkawa: Phys. Today **52** (1999) 33.

[5] M. Johnson and R. H. Silsbee: Phys. Rev. Lett. **55** (1985) 1790.

[6] F. J. Jedema, H. B. Heersche, A. T. Filip, J. J. A. Baselmans, and B. J. van Wees: Nature **416** (2002) 713.

[7] M. Johnson, B. R. Bennett, M. J. Yang, M. M. Miller, and B. V. Shanabrook: Appl. Phys. Lett. **71** (1997) 974.

[8] F. G. Monzon, M. Johnson, and M. L. Roukes: Appl. Phys. Lett. **71** (1997) 3087.

[9] Th. G. S. M. Rijks, S. K. J. Lenczowski, R. Coehoorn, and W. J. M. de Jonge: Phys. Rev. B **56** (1997) 362.

[10] G. Schmidt, D. Ferrand, L. W. Molenkamp, A. T. Filip, and B. J. van Wees: Phys. Rev. B **62** (2000) R4790.

[11] X. Lou, C. Adelmann, S. Crooker, E. Garlid, J. Zhang, K. Reddy, S. Flexner, C. Palmstrom, and P. Crowell: Nature Physics, **3** (2007) 197.

[12] T. Inokuchi, T. Marukame, M. Ishikawa, H. Sugiyama, and Y. Saito: Appl. Phys. Express **2,** (2009) 023006.

[13] O. M. J. van't Erve, A. T. Hanbicki, M. Holub, C. H. Li, C. Awo-Affouda, P. E. Thompson,

and B. T. Jonker: Appl. Phys. Lett. **91** (2007) 212109.

[14] T. Sasaki, T. Oikawa, T. Suzuki, M. Shiraishi, Y. Suzuki, and K. Noguchi: IEEE Trans. Magn. **46** (2010) 1436.

[15] S. Datta and B. Das: Appl. Phys. Lett. **56** (l990) 665.

[16] E. I. Rashba: Fiz. Tverd. Tela (Leningrad) **2** (1960) 1224 [Sov. Phys. Solid State **2** (1960) 1109], Y. A. Bychkov and E. I. Rashba: *J. Phys. C* **17** (1984) 6039.

[17] Y. Sato, T. Kita, S. Gozu, and S. Yamada: J. Appl. Phys. **89** (2001) 8017.

[18] H. Choi, T. Kakegawa, M. Akabori: T. Suzuki, and S. Yamada: Physica E **40** (2008) 2823.

[19] Y. Sato, S. Gozu, T. Kita, and S. Yamada: Jpn. J. Appl. Phys. **40** (2001) L1093.

[20] M. Akabori, K. Suzuki and S. Yamada: Journal of Superconductivity: Incorporating Novel Magnetism, **18** (2005) 367.

[21] H. Choi, A. Nogami, T. Kakegawa, M. Akabori, and S. Yamada: Physica E **40** (2008) 1772.

[22] H. C. Koo, H. Yi, J.-B. Ko, J. Chang, S.-H. Han, D. Jung, S.-G. Huh, and J. Eom: Appl. Phys. Lett. **90** (2007) 022101: H. C. Koo, J. H. Kwon, J. Eom, J. Chang, S. H. Han and M. Johson: Science, **325** (2009) 1515.

[23] H. C. Koo, J. H. Kwon, J. Eom, J. Chang, S. H. Han: J. Magnetism and Magnetic Materials, **320** (2008) 1436.

[24] S. V. Iordanskii, Yu. B. Lyanda-Geller, and G. E. Pikus: JETP Lett. **60** (1994) 206.

[25] M. I. D'yakanov and V. I. Perel': Zh. Eksp. Teor. Fiz. **60** (1971) 1954 [Sov. Phys. JETP **33** (1971) 1053].

[26] M. Ciorga, C. Wolf, A. Einwanger, M. Utz, D. Schuh, and D. Weiss: AIP ADVANCES **1** (2011) 022113.

[27] D. J. Monsma and S. S. P. Parkin: Appl. Phys. Lett. **77** (2000) 720.

[28] S. Takahashi and S. Maekawa, Phys. Rev. **B67** (2003) 052409.
[29] T. Kimura, Y. Ohtani and J. Hamrle: Phys. Rev. **B73** (2006) 132405.
[30] T. Kimura, J. Hamrle and Y. Ohtani: Phys. Rev. **B72** (2005) 014461.
[31] J. Schliemann and D. Loss: Phys. Rev. **B68** (2003) 165311.

Figure Captions

Figure 1 (Color) (a) An optical microscope image of fabricated SV device. Note that three $Co_{0.8}Fe_{0.2}$ electrode pairs (white lines) are formed near the center of the device mesa structure. (b) Schematic diagram of SV device with NLSV measurement ($R_{NL} = V_{NL}/I_{NL}$) and three-terminal measurement ($R_{3T} = V_{3T}/I_{3T}$) geometries. Since we regard R_{3T} as an interface resistance R_I, we use this R_{3T} for the resistance-area product (R_IA) evaluation.

Figure 2 (Color) (a) The R_{NL} curves as a function of B at 1.5 K obtained in the three samples having different L ranges. The plots correspond to L = 1 (bottom), 3 (middle) and 8.5 μm (top). The solid and dashed curves represent up-sweep and down-sweep signals, respectively. (b) The typical I-V characteristics observed in $Co_{0.8}Fe_{0.2}/In_{0.75}Ga_{0.25}As$ interface at 1.5 K and B=0 by the 3T geometry. The solid and dashed lines correspond to 3 μm- and 1 μm-long $Co_{0.8}Fe_{0.2}$ electrodes, respectively. The slope of the lines give the $R_{3T} = R_I$ used for the R_IA evaluation.

Figure 3 (Color) (a) Comparison between R_{NL} signal difference ($R_{NL(up)} - R_{NL(down)}$, black) and R_{3T} signal differences ($R_{3T(up)} - R_{3T(down)}$, green and blue) of the two FM electrodes, which are adopted instead of the AMR signals to analyze magnetization process for the electrodes. (b) Magnitude of R_{NL} difference, $\Delta R_{NL} \propto |R_{NL(up)} - R_{NL(down)}|$ (see text) as a function of L. The results of three samples (different symbols) are plotted together.

Figures

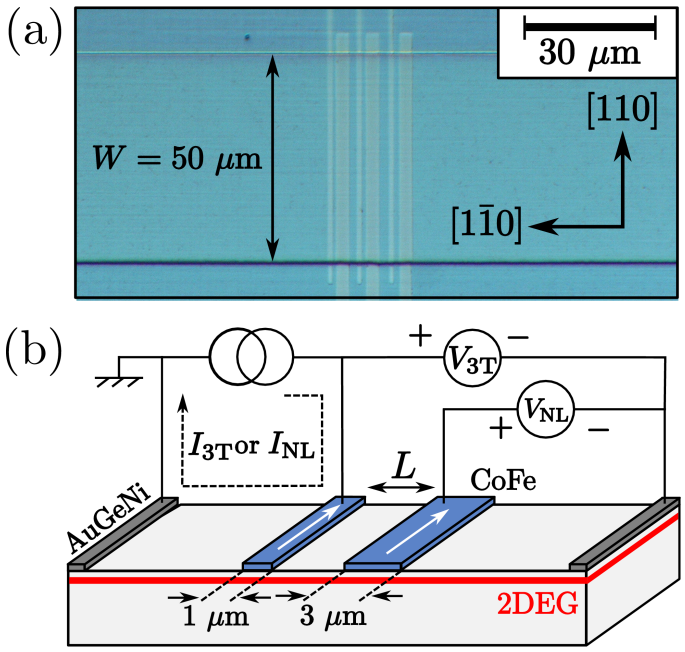

Figure 1 (Color)

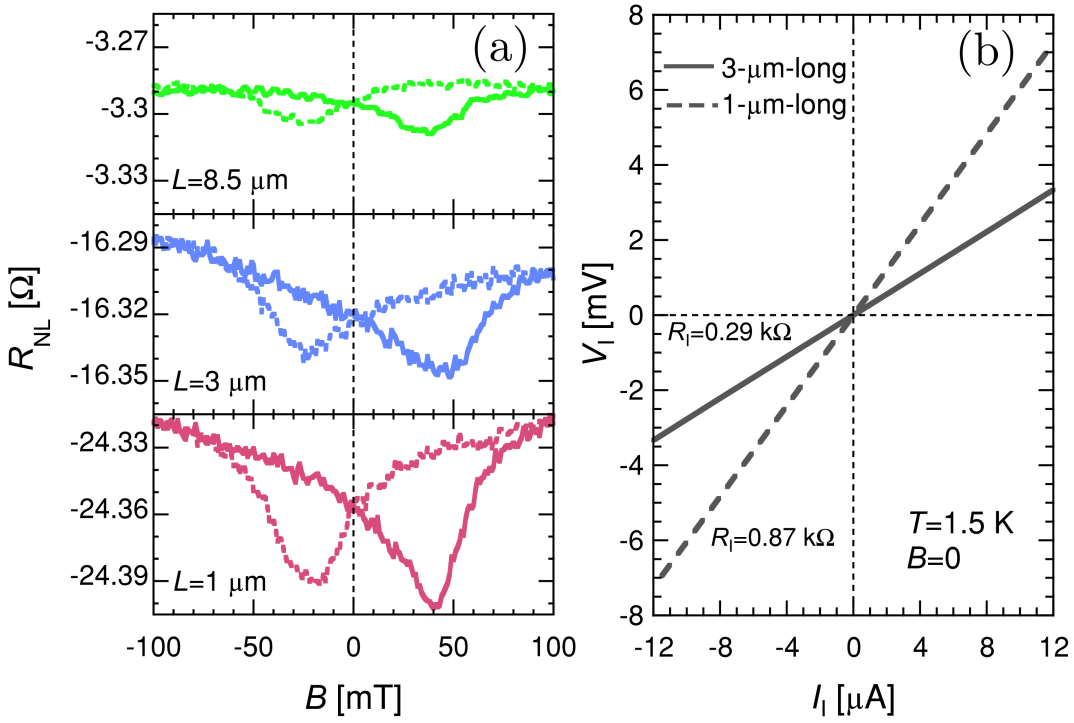

Figure 2 (Color)

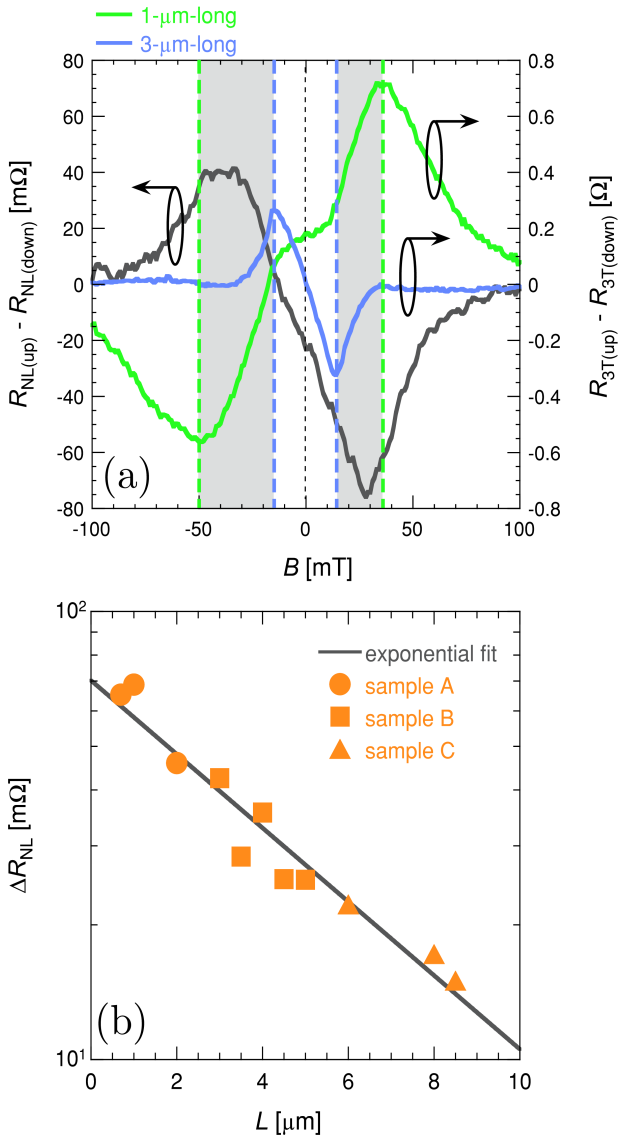

Figure 3 (Color)